Journal of Materials Chemistry A

Accepted Manuscript

ROYAL SOCIETY OF CHEMISTRY

www.rsc.org/materialsA

Journal of Materials Chemistry A

ARTICLE

Facile access to versatile hydrogel via interface-directed frontal polymerization derived from magnetocaloric effect

Received 00th January 20xx,
Accepted 00th January 20xx

DOI: 10.1039/x0xx00000x

www.rsc.org/

Chao Yu, Cai-Feng Wang,* Su Chen*

Stimuli-responsive hydrogels that are capable of adjusting to people's demand depending on environmental changes have attracted tremendous interest in recent years. To achieve flexibility for applications, multiresponsive smart materials are highly esirable, while it is still a great challenge to incorporate three or more responsive elements in one polymeric system. Herein, taking advantage of magnetocaloric effect, we developed an interface-directed frontal polymerization to achieve the fabrication of versatile hydrogel within 5 min. The as-prepared hydrogel shows the auto-healing without the assistance of any external stimuli and the addition of graphene oxide (GO) can lead to better performance in toughness and healing efficiency. Moreover, the combination of chemical, pH, thermal and electrical responses takes place within the resultant copolymer that exhibits different swelling and bending behavior towards various external changes. These features might provide the synthetic hydrogels great promise for a diverse range of applications.

Introduction

The living organisms are able to self-regulate by biomacromolecules that respond to variations in local environment. Mimicking nature, many synthetic materials have been developed which can undergo changes on receiving external signals. Such materials are considered as "intelligent" materials showing useful applications in biology and medicine.[1-4] Of particular interest are responsive polymers, a class of soft and highly deformable materials that can respond to chemical, physical or biochemical stimuli.[5-7] Up to now, most responsive polymers reported are single stimulus or dual-stimuli systems. Wu et al. grafted cellulose nanocrystals with P(N-isopropylacrylamide) to obtain thermo- and fluorescent-responsive polymer brush.[8] Higushi et al. synthesized electro- and photo-responsive metallo-supramolecular polymer based on the metal–ligand or metal–metal interactions.[9] Zhang et al. reported a covalent dynamic gel based on reversible acylhydrazone and disulfide bonds, which exhibited both redox- and pH-responsive behaviours.[10] Bai et al. prepared thermal- and chemical-responsive polymer networks through the cross-linked reaction of P(vinyl butyral) and hexamethylene diisocyanate.[11] Very recently, several versatile hydrogels with a combination of three or more stimuli-responsive functionalities have also been achieved.[12-13] In our previous work, we developed triple stimuli-responsive, i.e., thermo-, pH-, and metal ion-responsive copolymers based on poly(*N*-vinylimidazole-*co*-methacrylic acid).[14]

Herein, we combined 2-hydroxypropyl acrylate (HPA), 1-vinyl-2-pyrrolidinone (NVP) and graphene oxide (GO) to synthesize quadruple stimuli-responsive and auto-healing hydrogel through the implementation of interface-directed frontal polymerization (IDFP). This work possesses the following characterisitcs: (1) developing a new mode of frontal polymerization, IDFP. We created an oil/water biphase interface-directed synthetic pathway that the oil phase serves as trigger and water phase as reactor, offering a tractable preparation to obtain targeted products in minutes. In this case, magetocaloric effect was employed to assist the ignition process in the oil phase, thereby making IDFP noncontact and energy-efficient; (2) exploring new self-repair hydrogel. In the majority of the self-healable polymer systems, the repair of macroscopic fracture requires the input of external stimuli, and challenges remain for the preparation of auto-repair materials which are more desirable for applications. The IDFP-prepared hydrogel P(HPA-*co*-NVP) (**G-1**) shows auto-healing capacity, and it exhibits better wound-repair and mechanical performance after the introduction of GO; (3) realizing the incorporation of quadruple stimuli-responsive functionalities in a single polymer system. The as-prepared hydrogel can convert chemical, pH, thermal and electrical signals into spontaneously conformational changes. Moreover, the hydrogel shows different swelling capacity and electric bending behavior to various tastes like saltiness, sourness, sweetness, and umami, allowing it potentially useful as smart tongue-like sensor. This work may demonstrate a strategy that

[a] C. Yu, C. F. Wang and Prof. S. Chen

State Key Laboratory of Materials-Oriented Chemical Engineering and College of Chemistry and Chemical Engineering
Nanjing Tech University (the former: Nanjing University of Technology)
Nanjing 210009 (P. R. China)
Fax: (+86) 25-83172258
E-mail: caifengwang@njtech.edu.cn; chensu@njtech.edu.cn

† Electronic Supplementary Information (ESI) available: [details of any supplementary information available should be included here]. See DOI: 10.1039/x0xx00000x

can be extended to fabricate a series of smart versatile materials with desired performance.

Experimental

Material

2-hydroxypropyl acrylate (HPA), 1-vinyl-2-pyrrolidinone (NVP), *N*,*N*'-methylenebisacrylamide (MBAA), and redox couple, ammonium persulfate (APS)/N,N,N',N'-tetramethylethylenediamine (TMEDA) were purchased from Aldrich and used as received. N,N-dimethylformamide (DMF), ethanol, chloroform, citric acid (CA), gluconic acid (GA), sodium glutamate (SG), sodium chloride (SC), glucose (GLU) and superparamagnetic iron oxide nanoparticles (Fe_3O_4) (99.5%; 20 nm beads) were obtained from Aladdin-reagent Ltd. (ShangHai, China) and used without any further purification. Graphene oxide (GO) was fabricated as reported literature.[15-16]

Interface-Directed Frontal Polymerization (IDFP) of G-1

The IDFP of G-1 was performed as follows: a beaker was loaded with an appropriate amount of APS, HPA, NVP and MBAA in the presence of glycerol under ultrasound treatment. Then, the reductant TMEDA was poured into the mixed solution. A typical composition was glycerol = 20 %, APS = 0.4 wt%, [APS]/[TMEDA] = 1:4 mol/mol, MBAA = 0.01 wt%. The homogeneous mixture was transferred to a tailored glass text tube (15 ml; 10 mm diameter). For the sake of slowing bulk polymerization, the reactant was kept at room temperature. Finally, a solution of dimethylsilicone oil mixing with Fe_3O_4 (8 wt%) was put into the tube to form oil/water interface and an external magnetic field (450 kHz) was subsequently utilized to supply enough energy to excite the magnetic moment fluctuations until the formation of a front from the interface.[17-19] The whole noncontact magnetocaloric treatment process was only about 30 s and can be ready for the next set of experiments. Note that pot life, a period of time that the reagent can remain at ambient temperature before spontaneous polymerization was assessed by leaving the homogeneous mixture at the ambient temperature and observing the system visually when spontaneous polymerization would take place. At typical amount of component, our reacting system is inert at 23 °C and exhibits the pot life of nearly 2 days, whereas, it turns to be very reactive after triggered through external magnetic stimuli (450 kHz) for only several seconds.

IDFP of GO/G-1

To carry out the IDFP of GO/G-1, the same amount of each component as described in the preparation of G-1 above were vigorously mixed with GO (1 wt%) in a beaker until the mixture was dissolved. Then the homogeneous mixture was added into a test tube. Finally, the upper layer of the mixture was heated through the interface-directed reaction of IDFP until a flat hot propagating front commenced.

Velocity and Temperature Measurements

The front velocities were determined by measurement of the front position as a function of time. The straight line of the front position versus time is indicative of the occurrence of pure FP.[20-21] Temperature profiles as a function of time were confirmed by means of Fluke Ti30 IR thermal imager, which was located at a fixed point for measuring temperature (the position of 4.3 cm away from the free surface was chosen for consideration in this work). After complete reaction, the end-products were removed from the tube for further investigation.

Characterizations

Chemical Structure

Fourier transform infrared (FTIR) studies were carried out on a Nicolet-6700 spectrometer from Thermo Electron at room temperature. The powders were ground into a dry KBr disk. In all cases, 32 scans at a resolution of 4 cm^{-1} were used to record the spectra.

Morphology Measurement

The surface microstructure of GO/G-1 without cross-linker were examined with a JEOL JEM-2100 TEM. A drop of sample solution was placed on a lacey carbon film that was left to dry before being transferred into the TEM sample chamber. The morphology of the cross section of G-1 prepared by IDFP was investigated by SEM with a QUANTA 200 (Philips-FEI, Holland) at 30.0 kV. G-1 used for SEM measurement were cut to expose their inner structure.

Thermal stability measurement

The thermal stability experiments were performed using a thermogravimetric analysis (NETZSCH STA 449F3, Germany). The samples were combusted in N_2 at the temperature ranging from 0 to 800 ^{o}C (10 ^{o}C/min).

Swelling Measurement

The swelling properties of the obtained polymers were determined by gravimetric analysis. Samples were stringently weighed and immersed into an excess amount of water or organic solvent at room temperature. At specified intervals of time, the samples were taken out to wipe off the excess water or organic solvent and weighed, and then returned to the swelling medium again. The experiment was continued until a constant weight of swollen samples was attained. The swelling ratio of as-prepared samples was calculated by the following equation:

Swelling ratio = $(W_s – W_d)/W_d \times 100$ %

Here, W_s and W_d are the mass of the swollen and dry gel, respectively. Three parallel measurements had to be performed to ensure reliable data.

Mechanical Testing

SANS CMT6203 testing machine was employed to perform the mechanical tensile stress versus strain experiments at ambient temperature. The mechanical properties of cylindrical samples (10 mm diameter) were achieved at a crosshead speed of 10 mm/min and the initial length between jaws was controlled at 50 mm. For reproducibility, each measurement was repeated at least three times and the values were averaged.

Healing of Versatile Hydrogels

For the self-healing tests, two freshly separated section of polymer hydrogels were stuck together and pressed for ca. 1 min. The rejoined sample was left to repair themselves for 24 h at room temperature without any external stimuli. Finally, stress-strain tests were carried out to assess the healing degree of the samples in different HPA/NVP weight ratios. Moreover, IR images of the healing process were performed on a Thermo Scientific Nicolet iN10 infrared microscope equipped with a liquid nitrogen cooled MCT detector (Thermo Electron Corporation, USA). IR microscopy data were collected using reflection mode. IR spectra were captured using an aperture size of 50 µm by 50 µm and were recorded over a range of 650-4000 cm^{-1}. An analysis of the IR microscopy data was performed using OMNIC picta software (Thermo Electron Corporation, USA).

Fluorescence Response of G-1 toward Temperature

The studies of fluorescence response toward temperature were carried out by immersing the plates of G-1 polymer hydrogels in the corresponding aqueous solutions (20 to 60 °C) for 12 h. Then the G-1 plates were taken out from solution and photoluminescence (PL) spectra of G-1 were measured on a Varian Cary Eclipse spectrophotometer equipped with a Xe lamp at room temperature. The excitation wavelength was set at 370 nm, the tube voltage was 450 eV, the excitation and emission slits were 5 nm. Ten parallel measurements were performed to ensure reliable data.

Bending Behavior in a DC Electric Field

All test samples were immersed in different molar concentrations of CA, GA, SG, SC and GLU aqueous solutions respectively prior to the electric-sensitivity measurements. After 24 h, the gels were taken out and cut into 20 × 2 × 2 mm strips prior to use. A testing solution was poured into a transparent PMMA cell equipped with two parallel graphite electrodes. The space between the electrodes was fixed at 50 mm. The gel strip was positioned in the centre of cell with angle gauge beneath it and then a 25 V DC electric field was applied.

Results and Discussion

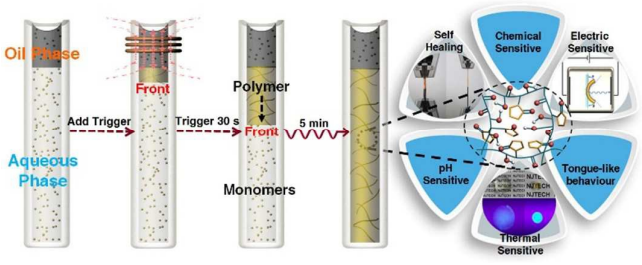

Figure 1. Schematic preparation of versatile hydrogels with self-healing and multistimuli-responsive functionalities via IDFP.

Synthesis of Versatile Hydrogels via IDFP

In this paper, we chose 2-hydroxypropyl acrylate (HPA), 1-vinyl-2-pyrrolidinone (NVP) and graphene oxide (GO) to synthesize P(HPA-*co*-NVP) (G-1) and GO/P(HPA-*co*-NVP) (GO/G-1) via interface-directed frontal polymerization (IDFP), as shown in Figure 1. A liquid-liquid interface can serve as an ideal platform to carry out various reactions.[22-25] Herein, we constructed an oil/water biphase interface, where the oil phase serves as trigger and water phase as reactor. Firstly, an appropriate amount of reactants was transferred to a tailored tube-like reactor (15 mL; 10 mm diameter). After triggered oil phase (dimethylsilicone oil mixing with Fe_3O_4) via external magnetic stimuli for only 30 s, the typical front commenced propelling from the biphase interface. Then no further energy was required in the next 5 min. G-1 and GO/G-1 were then successfully fabricated (see visually in Figure S2).

We conducted FTIR characterizations to analyse the chemical composition of G-1 and GO/G-1 prepared by IDFP, along with pure NVP and HPA. As shown in Figure 2a, O-H stretching vibrations, C=O stretching vibrations and -CH_2- bending vibrations appear for both NVP and HPA, peaking at 3450-3350 cm^{-1}, 1750-1700 cm^{-1} and 1450-1350 cm^{-1}, respectively. Bands at 1285 cm^{-1} can be assigned to C-N stretching vibrations and C–H (ring) in-plane bending in NVP. The observation of those above-mentioned peaks in the spectra of G-1 and GO/G-1 signifies the successful copolymerization between NVP and HPA in the process of IDFP. Moreover, GO/G-1 present a stronger and broader O-H absorption band, which may be attributed to the introduction of the functional groups of GO. Figure S5 shows the TGA analysis of G-1 and GO/G-1. Slight mass loss occurred upon heating above 60 ºC, presumably owing to the evaporation of adsorbed water and gas molecules. Then a major mass loss began at about 200 ºC to show huge degradation between 340–460 ºC. It is noted that G-1 exhibits higher thermal stability in the temperature range of 200–340 ºC than GO/G-1, which might be attributed to the degradation of functional groups of GO in the sample of GO/G-1.

To determine the pure IDFP without the occurrence of spontaneous polymerization (SP), we analysis the temperature profile of reaction process. As can be seen in Figure 2b, there is no variation of temperature before the front arrived at the fixed point, which appears as a horizontal part on the curve, indicating that pure IDFP without occurrence of SP. Moreover, corresponding frontal temperature values are obtained. Figure 2c-d shows the velocity and temperature of travelling front for the IDFP run. In the HPA/NVP ranging from 3:4 to 3:1 wt/wt, the frontal velocity (V_f) and temperature (T_{max}) of G-1 always maintain a higher value than that of GO/G-1. In terms of G-1, the V_f at HPA/NVP = 3:4, 3:3, 3:2 and 3:1 wt/wt are 0.73, 0.76, 0.94 and 1.15 cm/min, respectively. Analogous to this velocity trend, increasing the CD/VI from 3:4 to 3:1 wt/wt causes T_{max} to range from 96.0 to 113.0 °C. It comes out that T_{max} and V_f both increase as the HPA concentration steps up. Broadly, the variation of the HPA/NVP permits a facile tuning of T_{max} and V_f of IDFP under a nonadiabatic condition.

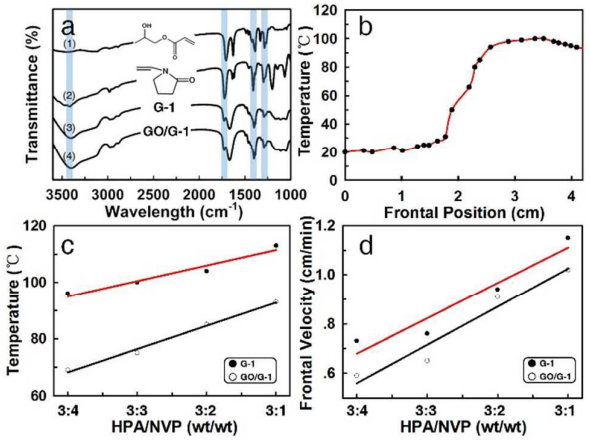

Figure 2. (a) FTIR spectra of (1) HPA, (2) NVP and (3) G-1 and (4) GO/G-1. (b) Typical temperature profile of G-1 prepared by IDFP. (c) Frontal velocity as a function of HPA/NVP weight ratio for G-1 and GO/G-1 via IDFP. (d) Frontal temperature as a function of HPA/NVP weight ratio for G-1 and GO/G-1 via IDFP.

Self-healing of Versatile Hydrogels Prepared by IDFP

The mechanical properties were studied systematically. As shown in Figure 3a-b, a set of stress–strain experiments were carried out for G-1 and GO/G-1 with different HPA/NVP ratios of 3:4, 3:3, 3:2, and 3:1 wt/wt, respectively. Basically, the tensile stress of all the samples is greatly reinforced with the increase in the HPA fragment. For instance, the tensile strength of G-1 with HPA/NVP ratio of 3:1 wt/wt (5.56 N) is nearly seven times that of the one with 3:4 wt/wt (0.88 N) and the elongation at break drops from 747.9 % to 401.4 % with the increase of HPA content. Moreover, the introduction of GO brings a noticeable impact on the mechanical strength of gels.[26-27] We can see that the tensile strengths of GO/G-1 are always higher than those of G-1, while there is a compromise on the elongation at break. The results reveal that the versatile hydrogels have good mechanical strength.

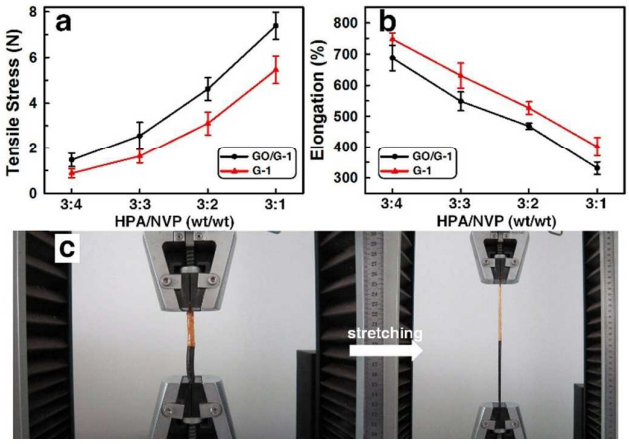

Figure 3. (a) Tensile stresses and (b) elongations versus different HPA/NVP ratios for G-1 and GO/G-1. (c) Stretching processes of a healed sample composed of one block of G-1 (yellow) and the other block of GO/G-1 (black) during the tensile measurements.

To estimate the self-healing property without external stimuli, the cylindrical polymer samples of 10 mm diameter were mechanically bisected and two halves were brought into contact for a given time. After several hours, the autonomic fusion of cut surface as well as self-healing occurred at ambient temperature. As visually seen in Figure 3c, the joint between the two blocks in the merged sample is strong enough to sustain vigorous stretching and the healed gel can be stretched from 5.0 cm to about 20.0 cm. To investigate the role of functional groups in the auto-healing process, we conducted spectroscopic analysis of incision area and corresponding healed area. As shown in Figure 4a-b, IR images exhibit chemical changes from the cut area to healed area of G-1, and directly illustrate the distribution of the oxygen-containing species of C=O (1751 and 1756 cm^{-1}, respectively) and –OH groups (3508 cm^{-1}) through color variation that red color means high intensity and blue color represents low intensity. The observation of oxygen-containing functional groups in IR spectra reveals that there is a large number of dangling C=O and –OH groups distributed along the freshly cut edges, while after complete healing reaction, hydroxyl and carbonyl groups become relatively uniform in the same place. This feature suggests that the intermolecular hydrogen bonding between hydroxyl moieties of HPA and the pyrrolidone moieties of the NVP enables strong adhesion across the rupture interface, thereby allowing the gels to weld (Figure 4c).[28]

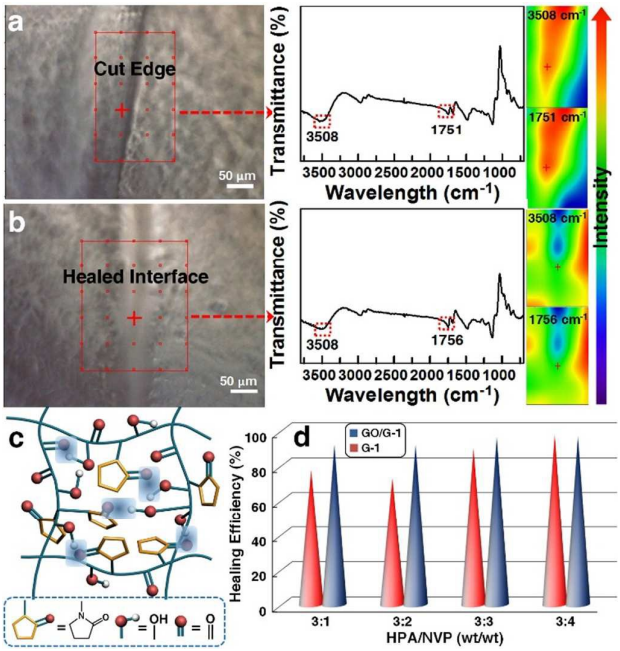

Figure 4. (a-b) Optical images (left), IR spectra (middle), and IR images (right) of G-1. (a) Cut edge; (b) Healed interface. (c) Schematic representation of healing process of IDFP-prepared polymer hydrogels. (d) Plots of healing recovery of the tensile modulus versus HPA/NVP ratios for G-1 and GO/G-1.

The optimal balance of hydrophobic and hydrophilic interaction of P(HPA-*co*-NVP) building block also endows the hydrogels with superior self-repair capacity. It comes out from Figure 4d that the healing efficiency increases as the fraction of NVP steps up, and finally peaks at HPA/NVP =3:4 wt/wt.

Taking G-1 for instance, the tensile modulus recovers from 77.3 % to 97.5 % with the HPA/NVP ranging from 3:1 to 3:4 wt/wt. Furthermore, GO/G-1 containing GO shows enhancement not only in the roughness but also in the spontaneous healing, and all of the healing degrees are above the 91.5 %. GO itself possesses self-healing ability that is the reconstruction of vacancy defects to heal the honeycomb structure through the rebonding of the dangling bonds surrounding the vacancy.[29] Meanwhile, the polar groups of the P(HPA-*co*-NVP) side chains interacted with the oxygen-containing groups of GO platelets in the form of hydrogen bonds.[30] Thus, GO/G-1 offers better healable performance based on the synergistic interplay between these two effects.

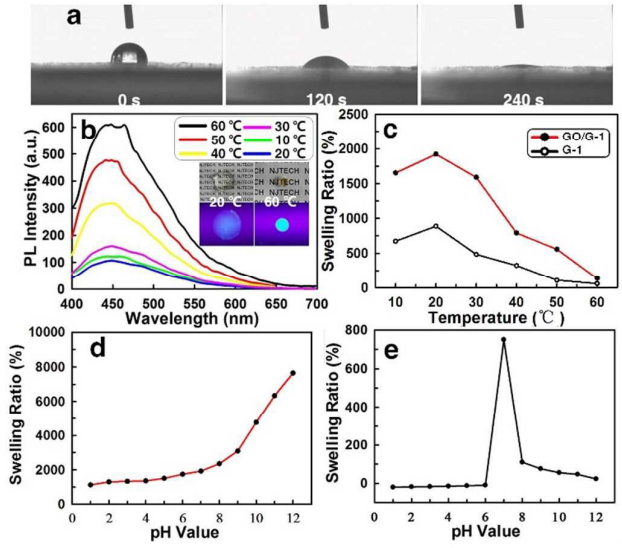

Figure 5. (a) water contact angles of G-1 versus time. ([HPA]/[NVP] = 3:4 wt/wt, MBA = 0.01 wt%, APS = 0.4 wt%, [APS]/[TMEDA] = 1:4 mol/mol). (b) PL spectra and the relative PL intensity of G-1 after swollen in aqueous solution at different temperature. (c) Equilibrium swelling ratio (ESR) as a function of temperature for G-1 and GO/G-1 with HPA/NVP = 3:3 wt/wt. (d-e) Swelling ratios as a function of pH values for (d) G-1 and (e) GO/G-1 at HPA/NVP = 3:3 wt/wt.

Thermal- and pH-sensitivity of Versatile Hydrogels Prepared by IDFP

The IDFP-prepared hydrogels show good swelling capacity which is thermal- and pH-sensitive. To evaluate the swelling capacity of polymer hydrogel, we firstly used water contact angle measurement to study water-absorbing ability of sample. It is more visible to observe the absorption rate of water by characterizing the dynamic water contact angles against residence time of water droplet at room temperature. Figure 5a shows the variation of water contact angle of G-1 versus time. The variation of G-1 is 100° at 0 second and in 2 minutes it plummet to 12.10°, which demonstrates the superior water absorption of G-1. The thermal sensitivity of G-1 and GO/G-1 is shown in Figure 5b-c, which is similar to the literature.[31] As shown in the inset of Figure 5b, molecular fluorescence is extremely sensitive to its microenvironment, namely temperature effect. As the temperature increases, the hydrogel swollen in the aqueous solution undergoes a deswelling process and shrinks to result in the enhancement in PL intensity.

We then assessed the pH dependence of the equilibrium swelling ratios (ESRs) for IDFP-prepared polymer G-1 and GO/G-1, as shown in Figure 5d-e. The swelling kinetics of G-1 immersed in aqueous solutions with different pH values (1-12) were thoroughly investigated (Figure 5d). G-1 doesn't swell much in the acid environment, while it shows a rapid swelling over a pH range of 7-12, with the ESRs of 1920 %, 2352 %, 3090.8 %, 4772 %, 6340 % and 7648.3 %, respectively. The explanation is that the hydrolysis of easter bond in the G-1 (P(HPA-*co*-NVP)) afford carboxyl groups that are in a ionization state at pH > 7, and the number of ionic charges on the backbone increases with the rise of pH of the solution. Consequently, G-1 could reach its fully swollen state at pH = 12. However, in Figure 5e, ESRs fall dramatically through the whole pH range as well as the addition of GO. This is due to the fact that GO and graphene sheets precipitate out of solution in an acid and alkali medium, which results from the protonation at pH 1-6 and salting out effect at pH 8-12.[32-33]

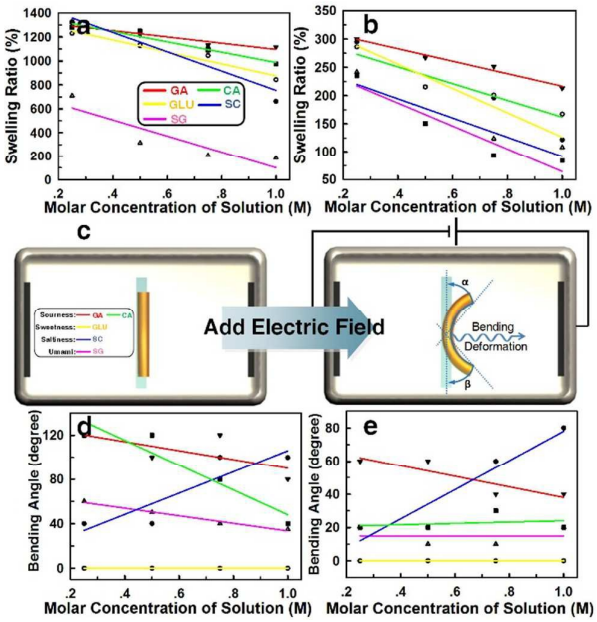

Figure 6. (a-b) ESRs of (a) G-1 and (b) GO/G-1 in the aqueous solutions of CA, GA, SG, SC and GLU, respectively. (c) Schematic representation for the electric-sensitive performance of IDFP-prepared polymer hydrogels. We defined the value of bending angle towards cathode as θ (θ = α + β). (d-e) Equilibrium bending angles of (d) G-1 and (e) GO/G-1 to an electric field in CA, GA, SC, SG, and GLU aqueous solutions, under 25 V electric field. Red, green, yellow, blue, and purple lines represent GA, CA, GLU, SC and SG, respectively.

Tongue-like Behavior of Versatile Hydrogels Prepared by IDFP

The IDFP-prepared polymer G-1 and GO/G-1 behave obviously different swelling behavior toward various taste solutions. As shown in Figure 6a, increasing the molar concentrations of taste solutions from 0.2 ~ 1.0 M make the ESRs of G-1 in GA, CA, GLU, SC and SG drop from 1305.7 to 1116.4 %, 1281.5 to 975.6 %, 1229.9 to 843.5 %, 1326.6 to 662.8 % and 709.7 to 184.0 %, respectively. This trend is consistent with that for

GO/G-1 in Figure 6b, which can be explained by the Flory's theory of the osmotic pressure. When the molar concentration grows, the osmotic pressure difference between the inside and outside of the polymer network decrease to some extent, along with the weak swelling performance of G-1 and GO/G-1 in corresponding solutions.

As a DC electric field is applied to strips of samples in GA, CA, GLU, SC and SG, G-1 and GO/G-1 behave excellent selective electro-sensitivity (as schematic illustrated in Figure 6c). Figure 6d-e presents the equilibrium bending angles (EBAs) of the G-1 and GO/G-1 strips in these five aqueous solutions, which the strips of samples bend toward the cathode in SG, SC, CA and GA (Glucose is not an electrolyte). Osmotic pressure is also related to the bending phenomenon of samples induced by the external electric field.[34] With the electric field is applied, the electric potential across the parallel plate electrodes gives rise to the non-uniform distribution of ionic concentrations, generating the unequal concentration differences between the interfaces near to the anode and cathode as well as the unequal osmotic pressure at both interfaces. Due to the negative charged group within the gels, the diffusive cations decrease near the anode, resulting the osmotic pressure at the interface of gels near the anode larger than that near the cathode, therefore, the gel on the anode side swells greater than that on the cathode side, leading to the bending toward the cathode.[35-36] The preliminary results suggest these hydrogels can in principle distinguish tastes like sourness (CA and GA), umami (SG), saltiness (SC), or sweetness (GLU), which might be extended to apply in food, beverage and pharmaceutical areas.

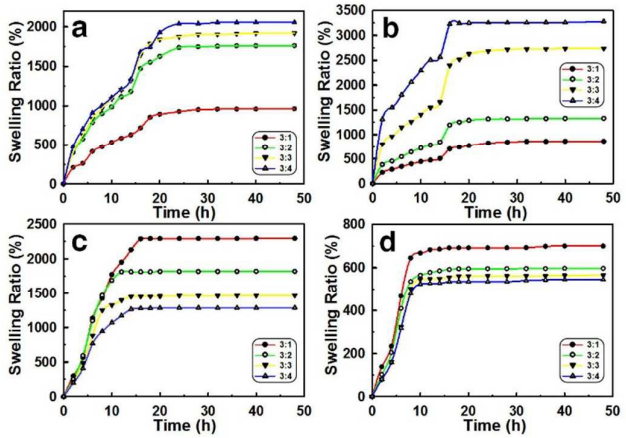

Figure 7. The swelling ratios of G-1 prepared by IDFP in different solvents: (a) water, (b) chloroform, (c) DMF and (d) ethanol at different HPA/NVP weight ratios of 3:1, 3:2, 3:3 and 3:4 wt/wt, respectively.

Chemical-sensitivity versatile hydrogels prepared by IDFP

We used gravimetric analysis to further investigate the swelling kinetics behavior of G-1 prepared under different HPA/NVP weight ratios. As seen in Figure 7, the swelling ratios witness a bullish trend with the elevated swelling time and the SRs of G-1 in DMF and ethanol move faster in the first 15 h. The swelling equilibrium for the whole system is achieved after 30 h of swelling time. As for ESR in H_2O and chloroform, increasing the hydrophilic NVP content lead to a noticeable improvement in the ESRs of G-1. Samples containing highest fraction of NVP (HPA/NVP = 3:4 wt/wt) exhibit maximum ESR data: 2056.9 % for H_2O and 3280.2 % for chloroform. On the contrary, the swelling behaviors of G-1 in DMF and ethanol are the exact opposite. The ESRs rise to their highest points at HPA/NVP = 3:1 wt/wt, which are 2292.7 % for DMF and 700.4 % for ethanol. G-1 with higher HPA content swell to a higher extent that can be ascribed to the relatively more lipophilic of HPA than NVP (Figure 8a). Therefore, the control of swelling capacity that is available by altering the weight ratio of HPA/NVP help to achieve targeted hydrophilic-lipophilic balance.

In Figure 8b-c, the SRs of GO/G-1 at HPA/NVP = 3:3 wt/wt clearly present the influence of the GO amount on the swelling capacity. Similarly, the SRs of GO/G-1 experience an upforward trend over swelling time, while after approximately 30 h, they begins to hover at corresponding stable values. As compared to the GO-free counterpart in Figure 8c, the ESRs of GO/G-1 fall behind in all four solvents. The swelling degrees of GO/G-1 in DMF and ethanol are close to those of G-1, while there exists a substantial discrepancy between two data for H_2O or Chloroform. It is a clear evidence that the introduction of GO may be the main factor contributing to the changes of ESRs. The above investigations suggest that IDFP is a procedure of converting monomer into polymer via a self-propagating reaction wave that continuously convert chemical energy into thermal energy and thus may lead to the reduction of GO.[37-38] As the hot front travels through the mixture, the exothermic chemical conversion occurs in a narrow reaction zone, where certain fraction of "oxo" functionalities are exfoliated from GO platelets, resulting in the formation of graphene structure. For this reason, hydrophobic graphene sheets formed in the GO/G-1 deteriorate the water affinity as well as cause the difference between the ESRs of G-1 and GO/G-1.

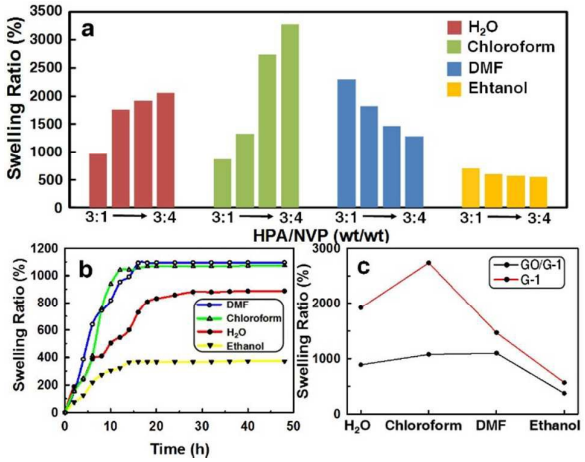

Figure 8. (a) The ESRs of G-1 prepared by IDFP in different solvents: water, chloroform, DMF and ethanol at different HPA/NVP weight ratios of 3:1, 3:2, 3:3 and 3:4 wt/wt. (b) The SRs of GO/G-1 prepared by IDFP in different solvents: water, chloroform, DMF and ethanol at HPA/NVP = 3:3 wt/wt. (c) The ESRs of G-1 and GO/G-1 prepared by IDFP in different solvents: water, Chloroform, DMF and ethanol at HPA/NVP = 3:3 wt/wt.

Conclusion

In conclusion, we demonstrate herein the first fabrication of quadruple stimuli-responsive hydrogel with self-repair capacity through the rapid interface-directed frontal polymerization (IDFP), which differs from the previous methods and materials. Once spatiotemporally ignited via the magnetocaloric effect, no additional energy or treatment is required for the following polymerization, and then the end-product can be obtained within minutes. The as-prepared versatile hydrogel P(HPA-*co*-NVP) shows automatic self-healing capacity, which can be adjusted by the suitable content of the HPA/NVP to offer an optimal healing efficiency based on hydrogen bonding. The introduction of GO could be contributed to maintain the healing degree hover around 91.5 %. Furthermore, the resultant polymer shows thermal-, pH-, electric- and chemical-sensitive shape changes, as well as various deformations toward sourness (CA and GA), umami (SG), saltiness (SC), and sweetness (GLU) potentially useful for artificial tongue-like sensing materials. The interesting development of method and material in this work provides a new insight into the rapid fabrication of smart versatile materials that is adaptable for various applications in such as biosensors, diagnostics, tissue engineering, and drug delivery.

Acknowledgements

This work was supported by the National High Technology Research and Development Program of China (863 Program) (2012AA030313), National Natural Science Foundation of China (21006046 and 21474052), Natural Science Foundation of Jiangsu Province (BK20131408), Priority Academic Program Development of Jiangsu Higher Education Institutions (PAPD), and Jiangsu Overseas Research & Training Program for University Prominent Young & Middle-aged Teachers and Presidents.

Notes and references

1 N. M. Alves, I. Pashkuleva, R. L. Reis and J. F. Mano, *Small*, 2010, **6**, 2208.
2 J. Kim, J. Yoon and R. C. Hayward, *Nat Mater*, 2010, **9**, 159.
3 G. Pasparakis, N. Krasnogor, L. Cronin, B. G. Davis and C. Alexander, *Chem Soc Rev*, 2010, **39**, 286.
4 L. Zhou, J. Li, Q. Luo, J. Zhu, H. Zou, Y. Gao, L. Wang, J. Xu, Z. Dong and J. Liu, *Soft Matter*, 2013, **9**, 4635.
5 M. A. C. Stuart, W. T. S. Huck, J. Genzer, M. Mueller, C. Ober, M. Stamm, G. B. Sukhorukov, I. Szleifer, V. V. Tsukruk, M. Urban, F. Winnik, S. Zauscher, I. Luzinov and S. Minko, *Nat Mater*, 2010, **9**, 101.
6 X. Yan, F. Wang, B. Zheng and F. Huang, *Chem Soc Rev*, 2012, **41**, 6042.
7 F. D. Jochum and P. Theato, *Chem Soc Rev*, 2013, **42**, 7468.
8 W. B. Wu, F. Huang, S. B. Pan, W. Mu, X. Z. Meng, H. T. Yang, Z. Y. Xu, A. J. Ragauskas and Y. L. Deng, *J Mater Chem A*, 2015, **3**, 1995.
9 M. Higuchi, *J Mater Chem C*, 2014, **2**, 9331.
10 P. Zhang, F. Y. Deng, Y. Peng, H. B. Chen, Y. Gao and H. M. Li, *Rsc Adv*, 2014, **4**, 47361.
11 Y. K. Bai, Y. Chen, Q. H. Wang and T. M. Wang, *J Mater Chem A*, 2014, **2**, 9169.
12 J. M. Zhuang, M. R. Gordon, J. Ventura, L. Y. Li and S. Thayumanavan, *Chem Soc Rev*, 2013, **42**, 7421.
13 P. Schattling, F. D. Jochum and P. Theato, *Polymer Chemistry*, 2014, **5**, 25.
14 H. Shao, C. F. Wang, J. Zhang and S. Chen, *Macromoleculars*, 2014, **47,** 1875.
15 D. Li, M. B. Muller, S. Gilje, R. B. Kaner and G. G. Wallace, *Nat Nanotechnol*, 2008, **3**, 101.
16 D. C. Marcano, D. V. Kosynkin, J. M. Berlin, A. Sinitskii, Z. Z. Sun, A. Slesarev, L. B. Alemany, W. Lu and J. M. Tour, *Acs Nano*, 2010, **4**, 4806.
17 C. Yu, C. F. Wang and S. Chen, *Advanced Functional Materials*, 2014, **24**, 1235.
18 B. Mehdaoui, A. Meffre, J. Carrey, S. Lachaize, L. M. Lacroix, M. Gougeon, B. Chaudret and M. Respaud, *Advanced Functional Materials*, 2011, **21**, 4573.
19 P. Nordblad, *Nat Mater*, 2013, **12**, 11.
20 J. A. Pojman, V. M. Ilyashenko and A. M. Khan, *J Chem Soc Faraday T*, 1996, **92**, 2825.
21 T. Hu, S. Chen, Y. Tian, J. A. Pojman and L. Chen, *J Polym Sci Pol Chem*, 2006, **44**, 3018.
22 S. Y. Yang, C. F. Wang and S. Chen, *J Am Chem Soc*, 2011, **133**, 8412.
23 L. R. Hou, Q. Zhang, L. T. Ling, C. X. Li, L. Chen, and S. Chen, *J Am Chem Soc*, 2013, **135**, 10618.
24 D. K. Beaman, E. J. Robertson and G. L. Richmond, *P Natl Acad Sci USA*, 2012, **109**, 3226.
25 Z. F. Li, W. Richtering and T. Ngai, *Soft Matter*, 2014, **10**, 6182.
26 C. L. Bao, Y. Q. Guo, L. Song and Y. Hu, *J Mater Chem*, 2011, **21**, 13942.
27 X. Huang, Z. Y. Yin, S. X. Wu, X. Y. Qi, Q. Y. He, Q. C. Zhang, Q. Y. Yan, F. Boey and H. Zhang, *Small*, 2011, **7**, 1876.
28 Y. Li, S. S. Chen, M. C. Wu and J. Q. Sun, *Adv Mater*, 2012, **24**, 4578.
29 D. Y. Kim, S. Sinha-Ray, J. J. Park, J. G. Lee, Y. H. Cha, S. H. Bae, J. H. Ahn, Y. C. Jung, S. M. Kim, A. L. Yarin and S. S. Yoon, *Advanced Functional Materials*, 2014, **24**, 4986.
30 H. P. Cong, P. Wang and S. H. Yu, *Chem Mater*, 2013, **25**, 3357.
31 Y. Fang, H. Yu, L. Chen and S. Chen, *Chem Mater*, 2009, **21**, 4711.
32 X. B. Fan, W. C. Peng, Y. Li, X. Y. Li, S. L. Wang, G. L. Zhang and F. B. Zhang, *Adv Mater*, 2008, **20**, 4490.
33 S. F. Pei and H. M. Cheng, *Carbon*, 2012, **50**, 3210.
34 T. Shiga and T. Kurauchi, *J Appl Polym Sci*, 1990, **39**, 2305.
35 Z. H. Zhang, X. F. Shi, X. Guo, C. F. Wang and S. Chen, *Soft Matter*, 2013, **9**, 3809.
36 D. Morales, E. Palleau, M. D. Dickey and O. D. Velev, *Soft Matter*, 2014, **10**, 1337.
37 H. L. Wang, J. T. Robinson, X. L. Li and H. J. Dai, *J Am Chem Soc*, 2009, **131**, 9910.
38 X. F. Gao, J. Jang and S. Nagase, *J Phys Chem C*, 2010, **114**, 832.

Table of Contents (TOC) graphic

Facile Access to versatile hydrogel via Interface-directed Frontal Polymerization derived from Magnetocaloric effect

Chao Yu, Cai-Feng Wang,* Su Chen*

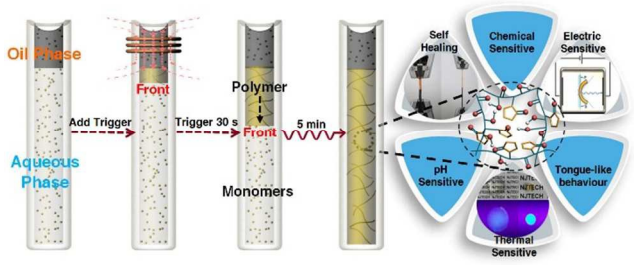

An interface-directed synthetic pathway is employed to offers a tractable preparation of versatile hydrogels in minutes. The resultant hydrogels show pH, thermal, electrical and chemical responsive shape changes as well as adjustable self-healing capacity.

This page is for Table of Contents use only.